Advanced DFN Models from Multi-Support Data for Underground Facilities

Romain Le Goc, Caroline Darcel, Philippe Davy

Symposium of the International Society for Rock Mechanics

Advanced DFN Models from Multi-Support Data for Underground Facilities

R. Le Goc[a]*, C. Darcel[a], P. Davy[b]

[a]Itasca Consultants SAS, 64 chemin des Mouilles, 69130 Écully, France
[b]Géosciences Rennes, CNRS, Université de Rennes 1, Campus de Beaulieu, 35042 Rennes Cedex, France

Abstract

Fractures have a significant impact on rock mass mechanical and hydraulic properties, which is a concern for rock engineering applications like excavation or repository design, support design, slope stability and caving in mines. To address this issue, a sound description of the fracturing pattern is required. DFN models are statistical models which define the density of fractures having given geometrical properties (size and orientation) and which include an intrinsic variability term. One of the main challenging task is to combine all available data. Data remain sparse and scarce and are acquired at different scales and from different support shapes and dimension (1D, 2D). We present a 3D modelling approach combining data from borehole logs, outcrop trace maps and tunnel walls mapping. It is applied to the Äspö site in Sweden, for which a large database is available, containing tens of thousands of records. Using stereological rules and assumptions about the underlying DFN scaling model, we are able to integrate all data to define the fracturing properties from the borehole scale (ten centimeters) to the repository scale (several kilometers). An advanced DFN modeling framework is applied, accounting for fractures mechanical interactions. This model has proved to be almost universal in crystalline rocks and reproduces, with very few parameters, the scaling properties of fractures. We show that this modelling framework better reproduces observations at all available scales and yields DFN, which structure and associated properties have a better consistency with natural cases than for simple DFN approaches.

© 2017 The Authors. Published by Elsevier Ltd. This is an open access article under the CC BY-NC-ND license (http://creativecommons.org/licenses/by-nc-nd/4.0/).
Peer-review under responsibility of the organizing committee of EUROCK 2017

Keywords: DFN; Modelling; Scale; Borehole logs; Fracture mapping

---

* Corresponding author. Tel.: +33-472180420; fax: +33-472180421.
  E-mail address: r.legoc@itasca.fr

1. Introduction

Studying fractured systems is a requirement for many industrial applications including nuclear waste deep repositories, geothermal energy exploitation in crystalline hard rocks and oil and shale gas extraction. In these fields, fractures are key factors for rock masses flow and mechanical properties. Fracture networks are complex systems arising from the physics of fracture development and from complex interactions between fractures. Because of this intrinsic complexity, fracture systems present the classical characteristics of complex systems with power-law scaling relationships [1]. This is now widely recognized from geological studies [2–4].

The major difficulty for defining Discrete Fracture Network (DFN) models is the limited amount and the nature of available data. Despite constant technical improvements, high-resolution measurements of fracture patterns are mostly limited to borehole and surface mapping, thus raising both under-sampling and stereological issues. The fracture system is defined at best from statistical distributions, which are the basic ingredients for interpolating local measurements at the site scale. The precise knowledge of these distributions, including scaling, is a critical issue for site modeling.

In this paper, the site-scale DFN model of the Äspö site in Sweden is revised in the framework of advanced DFN modelling. The approach initially proposed in [5] and further developed in [6] is used. For the Äspö site, a large database is available, which encompasses several ten thousand records of fractures from various supports (cored boreholes and tunnels). Both data types are analyzed and proper stereological relations are used to derive the corresponding 3D properties. The modelling assumptions are tested to check if they are consistent with the observations and define the characteristics of the fracturing properties.

2. DFN model characterization

In this section, the DFN model, the associated parameters and the stereological relations used to estimate these parameters from observed data are recalled.

2.1. DFN model parameters

A DFN model is a set of statistical laws that define the size, orientation and spatial distributions associated to a given fracture population. DFN models are characterized by their density distribution n(l, θ, ϕ, V), describing the number of fractures with respect to fracture size l and angles (θ, ϕ) in the domain V. Additional properties, such as aperture and/or transmissivity for flow modeling, must also be considered depending on the intended use of the DFN model.

Whereas fracture networks can be modeled as 2D structures organized in 3D, the sampling system is limited both in dimensionality (2D surfaces for outcrops and tunnels, 1D lines for boreholes) and size, entailing stereological and scaling issues, respectively. Stereological rules, which are model dependent, are used to correct the former. The latter require defining scaling functions in V and l, in order to extrapolate measures to the adequate range of scales. Power-law models are commonly used for this [2–4], such that:

$$n\left(l,\theta,\phi,V\right) = \alpha\left(\theta,\phi\right) \cdot l^{-a} \cdot V^{\frac{D}{3}}; \tag{1}$$

where $\alpha\left(\theta, \phi\right)$ is a density term that depends on fracture orientation, a is the power-law scaling exponent for fracture size (usually in the range 3–4), and D is the topological dimension of the fracture set (≤ 3). The distribution is defined from a minimum fracture length l_{min} up to a maximum one l_{max} which is potentially not defined (infinite or as large as the site size).

Davy et al. [4, 7] have shown that the "*Universal Fracture Model*" (UFM) DFN model is relevant for SKB Swedish sites. The UFM DFN model is a two power-laws model, with l_c the transition scale. The main advantage of the UFM framework is that it includes simplified mechanical rules to generate and propagate fractures, accounting

for fracture-to-fracture interactions. In these conditions, the two power-laws regimes naturally occur, which reduces the number of free parameters in the model. The corresponding density distributions write:

$$\begin{cases} n\left(l_{\min} \le l \le l_c\right) = \alpha_g \cdot l^{-a_g} \\ n\left(l_c \le l < l_{\max}\right) = \alpha_u \cdot l^{-a_u} \end{cases} \qquad . \tag{2}$$

In Eq. 2, α_u and a_u can be directly derived from the UFM modelling framework. Indeed, $a_u = 4$ is a natural property exhibited by the model and, from various analyses, $\alpha_u \in [3; 7]$ and $a_g \approx 3$ (see [4, 7]). A preliminary study, based on outcrop trace maps and lineament maps analyses on the Simpevarp area, located nearby the Äspö Site [5], yields values of $\alpha_u \approx 6.8$ and $a_g = 3.2$. In addition, l_c is between 1 and 12 m (Fig. 1).
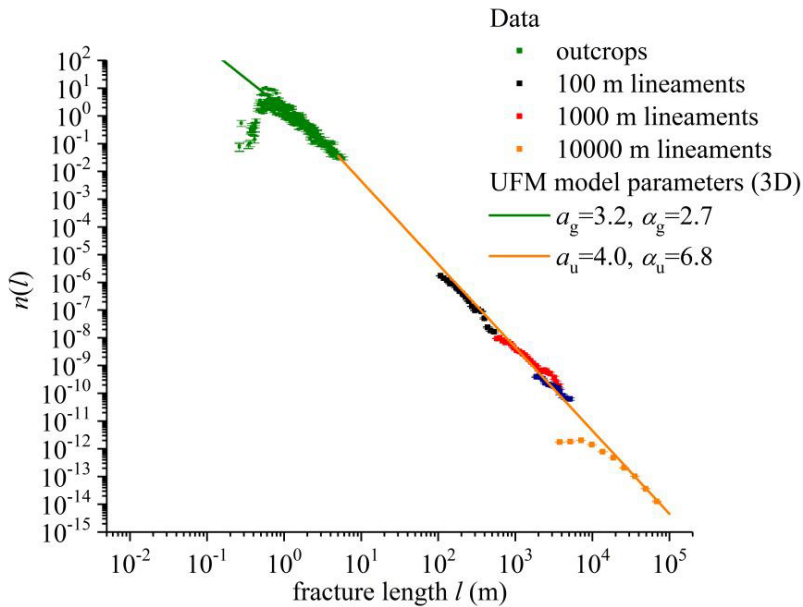

Fig. 1. Trace size distributions of surface data from the Simpevarp area and underlying models. Modified from [5].

With these conditions the DFN model mass density, defined as the total surface of fracture per unit volume, is equal to:

$$d_m\left(l_{min}, l_{max}\right) = \frac{\pi}{4}\left[\frac{\alpha_u l_c^{a_g - a_u}}{a_g - 3}\left(l_{\min}^{3 - a_g} - l_c^{3 - a_g}\right) + \frac{\alpha_u}{a_u - 3}\left(l_c^{3 - a_u} - l_{\max}^{3 - a_u}\right)\right]. \tag{3}$$

The DFN density d_m arises from the contribution of all length scales but is dominated by the minimum boundary of the system. The DFN density is thus strongly dependent on l_{min} and l_c.

In practice, fracture sampling is limited to core, surface mapping and tunnel walls mapping. Stereological relations are developed to relate the apparent DFN properties to the parent DFN model.

2.2. Stereology for cores

In boreholes, all fractures larger than the core diameter are sampled. In [9], the stereological relation between core data and DFN model are derived for the fractures which are fully intersecting the cores. This relation is an extension of the classical Terzaghi correction [8] applied to power-law models and accounting for finite-size effects. Equation 4 give the number of observed fracture intercepts along a core sample of length h and diameter d, with ϕ the angle between core and fracture pole:

$$n_{1d}\left(h,\phi\right)=\frac{\pi}{4}\cdot\alpha\left(\phi\right)\cdot h^{D_{3d}-2}\cdot f\left(a,l_{\min},d,l_{\max}\right)\cdot P\left(\phi\right).\tag{4}$$

$f(a, l_{min}, d, l_{max})$ and $P(\phi)$ are lengthy mathematical expressions not reproduced here (but available in [8]), with $P(\phi)$ the angular correction depending on $\cos(\phi)$. By combining Eq. 2 and Eq. 4, one can define the mass density and derive α_g or α_u depending on the conditions, and so determine l_c, since a_g, and a_u are either directly given by the UFM framework or inferred from simple analyses.

2.3. Stereology for tunnels

Tunnel trace maps are interesting data providing simultaneously density, orientation, and size information at depth, while borehole data provides only density and orientation and outcrops are available at the surface only.

Fracture traces in tunnels can be divided into two categories: fractures that transect the entire core, referred as Full Perimeter Intersection (FPI) fractures, and the others. For FPI, Eq. 4 can be used with d the tunnel diameter. In the second case, stereological analyses from fractures sampled along a cylinder are available in [10]. In the general case, the correction factor F (Eq. 11–16 in [10]) is dependent on the values of the fracture size l, the cylinder diameter T and the angle between fracture pole and the cylinder direction (noted α_M).

However, the fracture size is unknown and cannot be directly derived from the trace length. Nevertheless, in the case where $l < T \cdot \cos(\alpha_M)$ the correction factor depends only of α_M, the angle between the fracture intercept and the borehole, and writes (Eq. 14 of [10]):

$$F \cong \sqrt{\frac{1+\cos^2\alpha_M}{2}}\ .\tag{5}$$

For the present case, with a power-law size-distribution and $a_u = 4$, the number of large fractures is small and using Eq. 5 for all fractures only marginally impact the resulting density, as validated by direct 3D numerical simulations.

In addition, if the quantity of data is sufficient and if the mapping quality is strong enough, 2D trace length distributions can be derived, which provides additional information on the DFN characteristics (power-law exponent, density term).

3. Application to the Äspö site

The Äspö site is the research area of SKB for deep storage of nuclear waste in Sweden. In this area, the rock mass predominantly spans from granite to quartz diorite. Geological characterization of the Äspö Island and the nearby Simpevarp areas in Sweden started in the 1980s. Investigations at depth, with the Äspö Hard Rock Laboratory (HRL), have included the construction of a tunnel down to a depth of 460 meters for a total length of 3600 meters. Numerous boreholes have been drilled from the surface (for the longest ones) or directly from the tunnel. The selected database contains about 42000 fracture intercepts covering 9000 m of core and about 7000 fracture traces spread over 2800 m of the tunnel length. For most of the core datasets, fracture pole orientations are

only partially defined with only recording of acute angles. A picture of the site facility with tunnels and boreholes is given in Fig. 2.
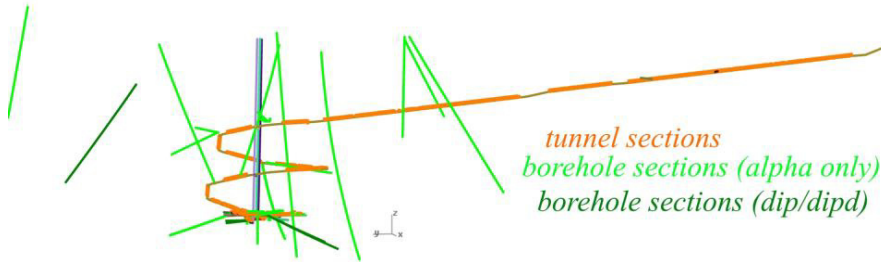

Fig. 2. Overview of datasets from the Äspö area. Tunnel sections with available data are emphasized. Boreholes with available core data are also plotted, with the distinction between cores with only acute angle and cores with pole orientation defined.

All available data of the Äspö site are thus used and the relevancy of the UFM at depth is assessed. In addition, the values of α_u and α_g, and consequently l_c (Eq. 2), will be derived from data.

3.1. Tunnel data analyses

The FPI fractures are first used to derive the corresponding d_m terms using Equations 2 and 4. Then, l_c is assumed to be smaller than the tunnel diameter, meaning that the FPI fractures are all in the second regime, to derive α_u. The whole tunnel is divided in sub-sections separated by the curved portions of the tunnel. Resulting values are given in Fig. 3.
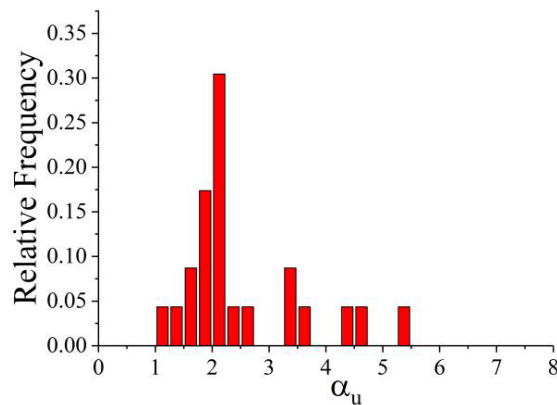

Fig. 3. Density term α_u derived from tunnel FPI data

The α_U values are slightly smaller than values obtained in previous studies based on outcrop trace maps. There are two possibilities explaining this: the density term of the UFM dense regime would be lower at depth, denoting an interesting aspect of the fracturing properties, or l_c is overestimated (it is supposed to be smaller than the tunnel diameter).

Tunnel data are further analyzed by studying the trace length distribution. Tunnel sections are grouped per depth and tunnel shape, leading to 3 series: n01to n10 (down to -335 m), n11 to n13 (down to -400) and n15 to n18 (down to -450 m). The trace size distributions of the three abovementioned series are plotted in Fig. 4, together with the outcrop trace size distributions from the Simpevarp site located nearby [5].
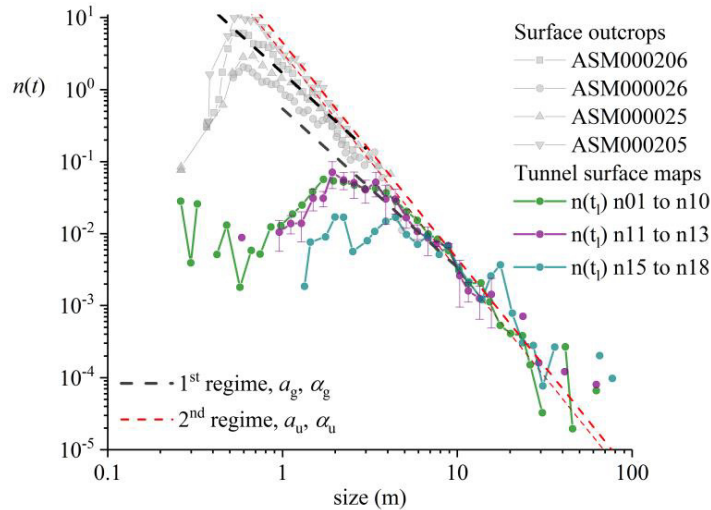

Fig. 4. Trace size distributions from Äspö tunnel data and some outcrops representative from the Simpevarp area. The second regime (short-dashed line) has $\alpha_u = 6.8$ and two first regimes are observed (long-dashed lines), one for outcrops and one for tunnel trace maps, yielding two possible l_c.

The second regime density term (in 3D) α_u is set to 6.8 according to the outcrop trace map study. It is an upper boundary for all distributions and seems relevant for tunnel trace size distributions, although slightly too large (consistently with Figure 3). Between 0.5 and 5 meters, the apparent fracture density assessed from the tunnel datasets is significantly below the one assessed from the surface datasets. It yields two different l_c values: $l_c \approx 3$ m for outcrop data and l_c between 8 and 15 m for tunnel data. There are two possible interpretations to explain this difference: sampling conditions are not the same between the surface and the depth, the resolution is lower at depth due to exposure conditions or fracturing is less dense at depth.

3.2. Core data analyses

At this scale, the two power-law regimes of the UFM contribute to the density of core data. The fracture frequency expected from the combination of two regimes below and above the transition scale l_c can be computed from Equation 4 by setting the appropriate boundaries and summing the contributions of the two regimes. a_g, a_u and α_u are set to 3.2, 4.0 and 6.8, respectively, according to Figure 4 and [5]. With these parameters fixed, Equation 4 can be used to estimate l_c as a function of the observed fracture frequency. The resulting values, calculated for each available borehole, are given by Fig. 5.

In most cases, l_c values are compatible with a UFM fracture model, with l_c covering a wide range between 1 and 10 m (to possibly 17 m). All these values are consistent with the interpretations of tunnel and outcrop data. Borehole data are rather dispersed, since boreholes are long and can possibly cross several fracture domains. In addition, boreholes are mainly dependant on fractures with sizes close to the borehole diameter (here 0.08 m), which properties likely are more heterogeneous than the properties of fractures with a larger size, dominating the properties of outcrop and tunnel wall trace maps.
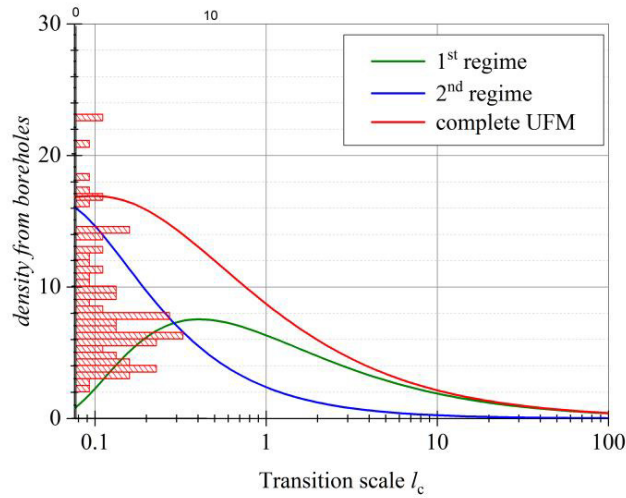
Fig. 5. Relation between the densities derived from borehole data and the UFM l_c (top line). The contribution of the two power-law regimes is also plotted (middle and bottom lines for the 1st and 2nd regime, resp.). The histogram of densities measured on Äspö boreholes is given on the left-hand side of the picture, allowing to estimate the corresponding l_c.

3.3. Synthesis

Fig. 6 summarizes all results. In general, tunnel data are consistent with l_c values between 8 and 15 m (for $\alpha_u = 6.8$) while surface data predicted l_c between 1 and 10 m. There is possibly a decrease of fracture density at depth compared to the surface, which would explain these differences.

Borehole data are consistent with l_c values between 1 and 17 m (for $\alpha_u = 6.8$), covering the range of both surface data and tunnel data. As a general conclusion, in-depth data are compatible with the UFM modelling framework, yielding l_c close to the one obtained with surface data. In addition, the current interpretation seems to show that there is a decrease of fracturing density at depth compared to the surface.
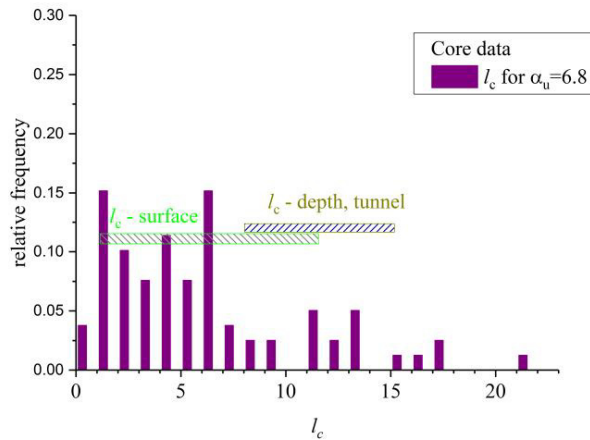

Fig. 6. Histograms for l_c computed from the core data with l_c, derived from outcrop trace maps and tunnel trace maps superimposed.

4. Conclusions

A series of stereological rules is applied to properly analyse 1D and 2D data from various support (core logs, outcrop trace maps, tunnel wall traces). These relations are used to derive the parameters of the DFN model. The UFM DFN modelling framework is used here to interpret data but the stereological relations are also suitable for classical power-law models. However, unlike classical models, the UFM framework yields, by construction, two power-law regimes, spatial correlation of fractures and requires almost no calibration. It is therefore a more robust approach.

After a review of accessible data in Äspö, several datasets are defined from borehole sections and tunnel sections suitable for analyses. Borehole densities and tunnel densities at depth are both consistent with the UFM framework and the tunnel trace-size distributions also exhibit a two power-law regime. By considering that the dense regime has a density term of $\alpha_u = 6.8$, borehole densities are compatible with a transition scale l_c between 1 and 17 m and tunnel densities between 8 and 15 m. These values are close to the transition scale estimated from surface data in [5], with l_c between 1 and 10 m. In addition, the size distributions of tunnel traces show two regimes, with a transition scale at around 8–10 m, consistently with the size distributions obtained with outcrop traces.

References

[1] A-L Barabási, R. Albert, Emergence of Scaling in Random Networks, Science 286 (1999) 509–512.
[2] E. Bonnet, O. Bour, N. Odling, P. Davy, I. Main, P. Cowie, et al., Scaling of fracture systems in geological media, Reviews of Geophyics 39 (2001) 347–383.
[3] O. Bour, P. Davy, C. Darcel, N. Odling. A statistical scaling model for fracture network geometry, with validation on a multi-scale mapping of a joint network (Hornelen Basin Norway). Journal of Geophysical Research 107 (2002).
[4] P. Davy, R. Le Goc, C. Darcel, O. Bour, J-R. de Dreuzy, R. Munier, A Likely-Universal Model of Fracture Scaling and its consequence for crustal hydro-mechanics, Journal of Geophysical Research, 115 (2010).
[5] C. Darcel, P. Davy, R. Le Goc, J-R de Dreuzy, O. Bour, R-09-38 - Statistical methodology for discrete fracture model – including fracture size, orientation uncertainty together with intensity uncertainty and variability. Svensk Kärnbränslehantering AB (SKB); 2009.
[6] C. Darcel, P. Davy, R. Le Goc, Development of the Statistical Fracture Domain methodology, Application to the Forsmark site, SKB R-13-54, Svensk Kärnbränslehantering AB (SKB); 2013.
[7] P. Davy, R. Le Goc, C. Darcel, A model of fracture nucleation, growth and arrest, and consequences for fracture density and scaling, Journal of Geophysical Research 118 (2013) 1393–1407.
[8] R.D. Terzaghi, Sources of errors in joint surveys, Geotechnique, 15 (1965) 287–304.
[9] P. Davy, C. Darcel, O. Bour, R. Munier, J-R. De Dreuzy, A note on the angular correction applied to fracture intensity profiles along drill core, Journal of Geophysical Research 111(2006) B11408.
[10] M. Mauldon, J.G. Mauldon, Fracture sampling on a cylinder: from scanlines to boreholes and tunnels, Rock Mechanics and Rock Engineering 30 (1997) 129–144.